Liquid-Crystalline Copolyester/Clay Nanocomposites

Guangli Zhang, Cuihong Jiang, Chenyu Su, Hongzhi Zhang

Department of Polymer Science and Engineering, College of Chemistry and Molecular Engineering, Peking University, Beijing, 100871, People's Republic of China

ABSTRACT: A series of novel polymer–clay nanocomposites, that is, liquid-crystalline copolyester/montmorillonite (MMT) nanocomposites, were synthesized by the intercalation polycondensation of terephthalic acid, *p*-acetoxy benzoic acid, and 1,2-diacetoxy benzene in the presence of different organically modified montmorillonites (OMt's). The OMt's were prepared by the ion exchange of MMT with octadecylamine hydrochloride, *p*-aminobenzoic acid hydrochloride, or lysine hydrochloride. X-ray diffraction and transmission electron microscopy studies indicated that the inorganic cations in the MMT interlayers were already exchanged by organic onium ions and that the OMt intercalated with *p*-aminobenzoic acid or lysine was good for obtaining more delaminated clay nanocomposites. The glass-transition temperature and modulus of the nanocomposites increased compared with those of the pure polymer, whereas the isotropic temperature decreased. © 2003 Wiley Periodicals, Inc. J Appl Polym Sci 89: 3155–3159, 2003

Key words: polyesters; nanocomposites; polycondensation

INTRODUCTION

Nanocomposites derived from the intercalation of organic polymers into mica-type layered silicates have attracted considerable attention from the perspectives of both fundamental research and applications.[1–3] Polymer-matrix nanocomposites are a relatively new class of materials, with the particle size of the dispersed phase having at least one dimension of less than 100 nm.[4] In general, nanocomposites exhibit new and improved performance properties in comparison with the pristine polymers because of the nanoscale structure of the hybrids and the synergism between the polymer and the silicate.[5]

Montmorillonite (MMT) is a mica-type silicate that belongs to the smectite family. Its structure consists of two silica tetrahedral sheets sandwiching an edge-shared octahedral sheet of aluminum hydroxide. Stacking 1-nm-thick layers by weak dipolar van der Waals forces leads to interlayers or galleries between the layers.[6] Isomorphic substitution within the layers generates negative charges that are counterbalanced by cations residing in the interlayers. Although the natural forms of MMT usually contain hydrated inorganic cations (Na^+ and Ca^{2+}), ion-exchange reactions with organic cations (e.g., alkylammonium ions) can render normally hydrophilic MMT organophilic.[7]

MMT is interesting as a nanocomposite reinforcement because of two particular characteristics.[7] The first is the ability to alter the surface chemistry of MMT through ion-exchange reactions with both organic and inorganic ions at the interlayer sites; this allows access to a broad range of physicochemical properties. The second involves the high aspect ratio of the silicate particles and a plate morphology. The aspect ratio can be maximized by the dispersion of individual silicate layers within a solid or liquid matrix. In that case, the aspect ratio can be as high as 1000 or more. These two characteristics are, of course, interrelated because the ability to disperse the silicate layers in a polymer matrix, thereby maximizing their aspect ratio, is partially dependent on the chemical mature of the interlayer cation. Because of its hydrophilic behavior, MMT often must be chemically treated to make it organophilic and compatible with the polymer matrix.

Over the past few years, many polymer–clay hybrids, such as polyimide,[8] epoxy resin,[9–12] polystyrene,[13–15] polypropylene,[16] polycaprolactone,[7] and acrylic polymer,[17] have been prepared, and most of these polymer systems have been blended with alkylammonium MMT or pure MMT. Liquid-crystalline copolyester (LCP) is one commercially used high-performance polymer. Concerning the preparation of LCP–clay nanocomposites, Vaia and Giannelis[18] recently reported that nanocomposites obtained by intercalation between organically modified clay and thermotropic LCP in a nematic state resulted in a loss of liquid crystallinity for the polymer. The purpose of this study was to synthesize LCP–clay nanocomposites by the intercalation polycondensation of terephthalic acid, *p*-acetoxy benzoic acid, and 1,2-diacetoxy benzene in the presence of different organomontmorillonites (OMt's). Furthermore, the morphology of the

LCP–clay nanocomposites and their properties were characterized.

EXPERIMENTAL

Materials

Sodium MMT with a cation-exchange capacity of 80 mequiv/100 g and octadecylammonium-modified MMT (N-clay) were provided by the Institute of Chemistry at the Chinese Academy of Science (Beijing, China). All other chemicals were used as purchased without further purification.

Synthesis of OMt's

Sodium MMT (15.2 g) was dispersed in 750 mL of hot water (ca. 80°C). *p*-Aminobenzoic acid (2.466 g, 12 mmol) or lysine (0.901 g, 6 mmol) and concentrated HCl (1.6 mL) were dissolved in 250 mL of hot water and added slowly to the aqueous MMT suspension with vigorous stirring; the mixture was stirred for 4 h. The precipitate was collected, washed with hot water three times, and dried, and organophilic MMT intercalated with *p*-aminobenzoic acid or lysine was obtained. It was abbreviated A-clay or L-clay, respectively.

Preparation of the LCP–MMT nanocomposites

Terephthalic acid (0.08 mol), *p*-acetoxy benzoic acid (0.04 mol), and 1,2-diacetoxy benzene (0.08 mol) were mixed with a desired amount of the appropriate OMt (N-clay, A-lay, or L-clay) and heated at 245–250°C for 3–4 h with stirring under a nitrogen atmosphere. When no more acetic acid distilled out, the pressure was reduced to 0.1–0.2 mmHg, and the temperature was increased to around 270°C. After 4–5 h, a polymer–clay composite with a liquid-crystal polymer burnish was obtained. The LCP–MMT composite was
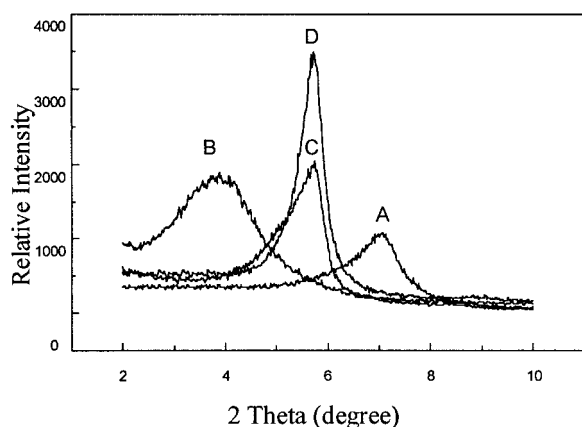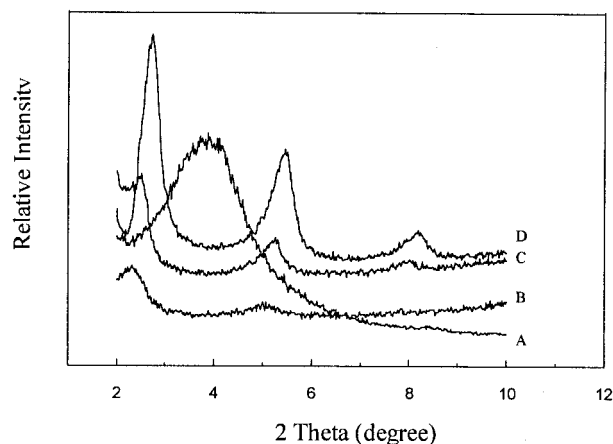
Figure 2 XRD curves of N-clay and its polymer hybrids: (A) N-clay, (B) LCPN-04, (C) LCPN-05, (D) LCPN-06.

dissolved in a mixture of chlorobenzene and tetrachloroethane (6:4 v/v), and this resulted in a stable, clear, and transparent solution.

CHARACTERIZATION

X-ray diffraction (XRD) was performed with a diffractometer (Rigaku, Japan) equipped with Cu Kα X-ray radiation. Transmission electron microscopy (TEM) micrographs were obtained with a transmission electron microscope (100CX, JEM, Japan) with an acceleration voltage of 100 kV. Polarized optical microscopy (POM) photomicrographs were taken on a Laborlux 12 Pol Leitz Wetzlar 350 polarized optical microscope (Leitz Corporation, Germany) with a hot stage (magnification, 360×). The thermoanalysis [differential scanning calorimetry (DSC)] was performed on a 2010 differential scanning calorimeter (TA Instruments, Inc., New Castle, DE) at a heating rate of 10°C/min. The dynamic modulus was measured on a Rheovibron DDV-II (Baldwin Co., Japan).

RESULTS AND DISCUSSIONS

Characterization of the OMt's

Organic cation intercalation plays a key role in polymer–clay nanocomposite formation by providing a hydrophobic environment for the intragallery adsorption of the polymer precursor. Our first goal was to synthesize an OMt suitable for forming the LCP/clay nanocomposites.

For comparison with N-Clay and MMT, A-Clay and L-Clay, containing amino and carboxylic acid reactive groups, were prepared. XRD patterns for various OMt's and pristine MMT are shown in Figure 1. The peaks of the curves correspond to the (001) plane diffraction of the clays. The OMt basal spacings increased to around 2.3 ($2\theta = 3.9°$), 1.6 ($2\theta = 5.72°$), and

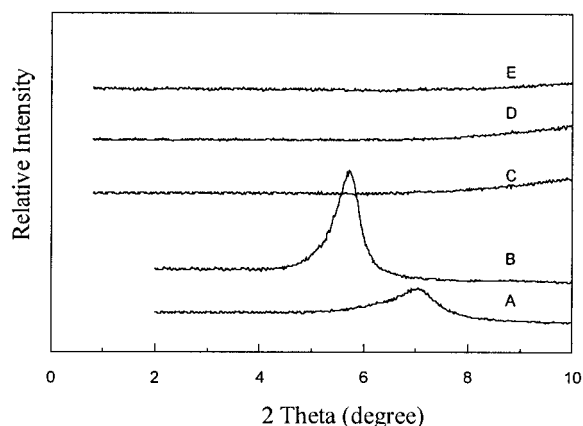**Figure 1** XRD curves of treated and untreated MMT: (A) MMT, (B) N-clay, (C) L-clay, and (D) A-clay.

Figure 3 XRD curves of A-clay and its polymer hybrids: (A) MMT, (B) A-clay, (C) LCPA-03, (D) LCPA-04, and (E) LCPA-05.

Figure 5 TEM micrograph of a cross section of an LCP–MMT nanocomposite containing 3 wt % A-clay.

1.5 nm ($2\theta = 5.98°$) for N-clay, A-clay, and L-clay, respectively; this can be compared with 1.2 nm ($2\theta = 7.02°$) for MMT. The increments of the OMt basal spacings indicated that the inorganic cations in the MMT interlayers were already exchanged by the organic onium ions. Because the molecular sizes of *p*-aminobenzoic acid and lysine are much smaller than that of octadodecylamine, the observed basal spacing of N-clay was somewhat greater than those of A-clay and L-clay. This result agreed with the conclusions of Lan et al.,[19] who studied bulky alkylamines of different lengths as intercalating reagents. In general, a greater basal spacing represents a higher capacity for intercalation polymerization. However, reactive groups such as carboxyl and amino groups in the silicate interlayers may play an even more important role in nanocomposite formation, as pointed out by Usuki et al.,[20] who used an OMt prepared by 12-aminolauric acid with pendent carboxyl groups in the galleries to initiate caprolactam polymerization; the
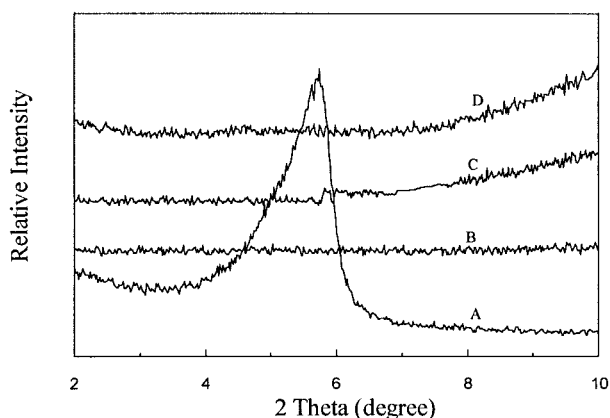
silicate layers of MMT were uniformly dispersed in the polymer.

Microstructure of the LCP–OMt nanocomposites

Composites formed with N-clay showed two separated XRD peaks at about 2.5 and 5° (Fig. 2). The broad peak of the initial N-Clay implied that N-clay had a series of arrays of silicate layers with basal spacings of 1.1 ($2\theta = 8°$) to 4.4 nm ($2\theta = 2°$). In the polycondensation process, monomers or polymer chains could diffuse into the larger basal spacing region of N-clay and expand the spacing to about 4 nm, but the partial region of smaller basal spacings was hardly intercalated and maintained spacings close to those covered by the diffuse peak of the original MMT [Fig. 1(A)]. It is noteworthy that composites formed with A-clay and L-clay exhibited no diffraction peaks in the 2θ range of 2–8° (Figs. 3 and 4). The absence of a Bragg scattering

Figure 4 XRD curves of L-clay and its polymer hybrids: (A) L-clay, (B) LCPL-03, (C) LCPL-04, and (D) LCPL-05.

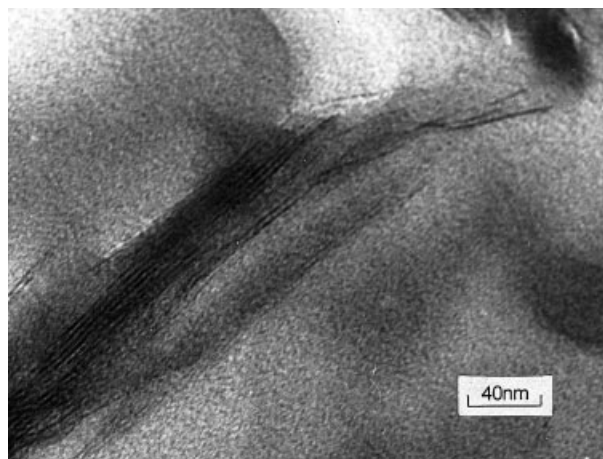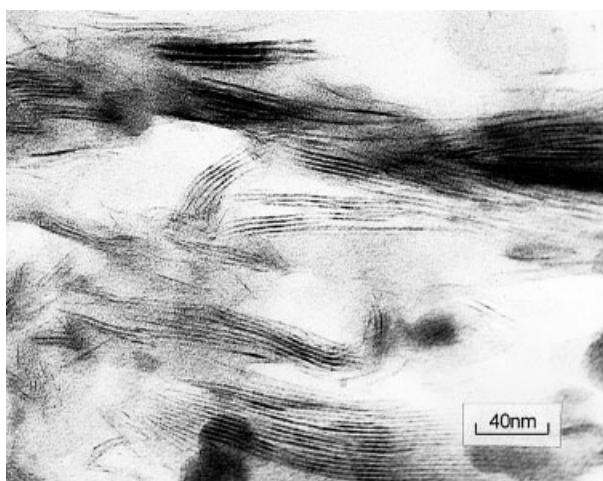**Figure 6** TEM micrograph of a cross section of an LCP–MMT nanocomposite containing 3 wt % L-clay.

TABLE I
Properties of the LCP–Clay Nanocomposites

No.	$[\eta]$ (d/Lg)	Clay (wt %)	DSC		POM	
			T_g (°C)	T_i (°C)	T_i (°C)	Modulus (GPa at 25°C)
LCP-1	0.48	0	121	282	275–280	0.93
LCPA-01		0.5	125	273	264–267	
LCPA-02	0.58	1	126	266	262–266	
LCPA-03	0.52	2	126	250	251–252	1.11
LCPA-04	0.55	3	126	257	258–260	1.00
LCPA-05	0.68	5	127	253	251–254	1.13
LCPL-01	0.52	0.5	123	276	270–275	
LCPL-02	0.58	1	125	271	265–273	
LCPL-03	0.55	2	125	265	258–263	1.00
LCPL-04	0.54	3	127	254	254–256	
LCPL-05	0.57	5	124	248	249–253	1.22
LCPN-01	0.32	0.2	123	274	265–268	1.05
LCPN-02	0.38	0.5	122	250	245–249	1.12
LCPN-03	0.31	1	122	249	241–246	1.15
LCPN-04	0.43	2	124	242	234–240	
LCPN-05	0.32	5	123	236	221–225	1.30
LCPN-06	0.36	10	122	235	220–225	1.73

peak seems to indicate that the clay tactoids were completely exfoliated by the intercalation polycondensation process. However, TEM images (Fig. 5) showed that in the composite containing 3 wt % A-clay, some of the silicate layers retained an ordered tactoid structure with a basal spacing of around 3 nm, others being more than 4 nm. A similar dispersion of clay platelets was observed for an L-clay composite (Fig. 6). Therefore, the original MMT was only delaminated into much smaller stacks, which contained far fewer silicate layers with interlayer distances in the nanometer range of 3 to infinity. The decrease and polydispersion of the silicate layer number in the stacks resulted in the absence of XRD peaks. Anyway, the OMt's intercalated with p-aminobenzoic acid and lysine were good for obtaining LCP–clay nanocomposites. The monomers and oligomers reacted with the pendant carboxyl and amino groups in the silicate galleries, continued to expand the interlayer distance as the polymerization progressed, and gave rise to the formation of more delaminated clay nanocomposites.

Transition temperatures and dynamic moduli of the LCP–MMT nanocomposites

The glass-transition temperature (T_g) of the LCP–MMT nanocomposites increased slightly compared with that of the pure polymer. The increase in T_g of the nanocomposites could be explained by the suggestion of Chang et al.,[21] whose article we read after this article had already been submitted to the journal editor for publication. The increase in T_g of these nanocomposites could be the result of two factors. First, the effect of small amounts of dispersed clay layers on the free volume of LCP was significant and influenced T_g of the LCP–MMT nanocomposites. The second factor concerns the confinement of the intercalated polymer
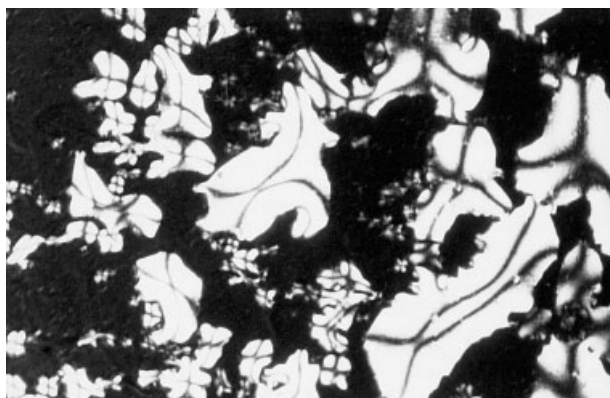

Figure 7 Photomicrograph of LCPA-01 at 248°C (crossed polarizers; original magnification, 360×).

Figure 8 Photomicrograph of LCPA-03 at 242°C (crossed polarizers; original magnification, 360×).
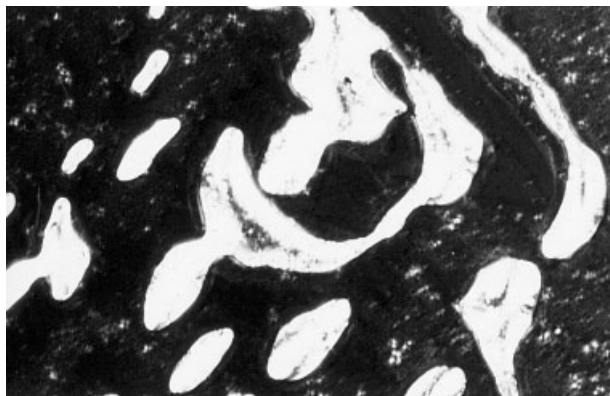
Figure 9 Photomicrograph of LCPA-05 at 240°C (crossed polarizers; original magnification, 360×).

chains within the clay galleries, which prevented segmental motions of the polymer chains.

The isotropic temperature (T_i) of the LCP–MMT nanocomposites decreased significantly with an increasing clay feed (Table I). For an A-clay composite with a clay content of 3%, the decrease in T_i reached 25°C. LCP chains were separated to a certain degree by inorganic silicate layers, which reduced the ordering ability of mesogenic units. This may be the main reason for the descent of T_i.

The nematic texture of the LCP–MMT nanocomposites could be observed in POM photomicrographs (Figs. 7 and 8). However, the schlieren texture of the nanocomposites became indistinct as the clay feed was increased. With a greater clay fed, the schlieren texture became more indistinct. For an A-clay nanocomposite with a clay content of up to 5 wt %, the schlieren texture in POM still could be observed at 258°C, although it was already discontinuous and indistinct (Fig. 9). This observation agreed with the suggestion of DSC analysis, that the high aspect ratio of intercalated MMT might cause a serious defect in the orientation in the liquid-crystalline phase. Therefore, the mechanism of disinclination in the nematic phase for the LCP–MMT nanocomposites was more complicated than that for pure LCP.

Dynamic mechanical testing showed that the moduli of the various composites obviously increased even with a very small amount of clay (e.g., 0.2 or 0.5%) and increased with the increment of the clay content.

CONCLUSIONS

OMt's intercalated by *p*-aminobenzoic acid hydrochloride and lysine hydrochloride with pendent carboxyl and amino groups in the silicate interlayers were syn-thesized. In comparison with the interlayer distance of octadecylammonium, their interlayer distances were further expanded during the intercalation polycondensation until the disappearance of XRD peaks in the 2θ range of 2–8°. However, the absence of peaks did not mean that the clay tactoids were completely exfoliated into individual thin layers, but the original MMT was delaminated into much smaller stacks, which contained far fewer silicate layers with interlayer distances in the nanometer range of 3 to infinity. Anyway, the OMt intercalated with *p*-aminobenzoic acid or lysine was good for obtaining the more delaminated clay nanocomposite.

The T_g value of the nanocomposites slightly increased compared with that of the pure polymer, whereas the T_i value decreased more significantly as the content of OMt increased, regardless of the kind of OMt used. The modulus of the nanocomposites obviously increased even with a very small amount of clay (e.g., 0.2 or 0.5%) and increased with the increasing content of OMt.

References

1. Messersmith, P. B.; Stupp, S. I. J Mater Res 1992, 7, 2599.
2. Okada, A.; Usuki, A. Mater Sci Eng C 1995, 3, 109.
3. Giannelis, E. P. Adv Mater 1996, 8, 29.
4. Komarneni, S. J Mater Chem 1992, 2, 1219.
5. Novak, B. M. Adv Mater 1993, 5, 422.
6. Grim, R. E. Clay Mineralogy; McGraw-Hill: New York, 1968.
7. Messersmith, P. B.; Giannelis, E. P. J Polym Sci Part A: Polym Chem 1995, 33, 1047.
8. Yano, K.; Usuki, A.; Okada, T.; Kurauchi, T.; Kamigaito, O. J Polym Sci Part A: Polym Chem 1993, 31, 2493.
9. Usuki, A.; Arimitsu, U.; Mizutani, T. U.S. Pat. 4,889,885 (1989).
10. Wang, M. S.; Pinnavaia, T. J. Chem Mater 1994, 6, 468.
11. Lan, T.; Pinnavaia, T. J. Chem Mater 1994, 6, 2216.
12. Kelly, P.; Akelah, A.; Qutubuddin, S.; Moet, A. J Mater Sci 1994, 29, 2274.
13. Vaia, R. A.; Isii, H.; Giannelis, E. P. Chem Mater 1993, 5, 1694.
14. Moet, A.; Akelah, A. Mater Lett 1993, 18, 97.
15. Chen, G.; Ma, Y.; Qi, Z. Acta Polym Sinica 2000, 5, 603.
16. Hasegawa, N.; Kawasumi, M.; Kato, M. Appl Polym Sci 1998, 67, 87.
17. Biasci, L.; Aglietto, M.; Ruggeri, G.; Ciardelli, F. Polymer 1994, 35, 3296.
18. Vaia, R. A.; Giannelis, E. P. Polymer 2001, 42, 1281.
19. Lan, T.; Kaviratna, P. D.; Pinnavaia, T. J. Chem Mater 1995, 7, 2144.
20. Usuki, A.; Kojima, Y.; Kawasumi, M.; Okada, A.; Fukushima, Y.; Kurauchi, T.; Kamigaito, O. J Mater Res 1993, 8, 1179.
21. Chang, J.; Seo, B.; Hwang, D. Polymer 2002, 43, 2969.